

# The somatic musculature of *Bryceella stylata* (Milne, 1886) (Rotifera: Proalidae) as revealed by confocal laser scanning microscopy with additional new data on its trophi and overall morphology

E.F. Wilts<sup>a,\*</sup>, W.H. Ahlrichs<sup>a</sup>, P. Martínez Arbizu<sup>b</sup>

<sup>a</sup>*Systematics and Evolutionary Biology, Department of Biology and Environmental Sciences, Carl von Ossietzky University Oldenburg, 26111 Oldenburg, Germany*

<sup>b</sup>*Senckenberg Research Institute, German Centre for Marine Biodiversity Research (DZMB), 26382 Wilhelmshaven, Germany*

Received 19 June 2009; received in revised form 10 August 2009; accepted 11 August 2009

Corresponding Editor: Sorensen

---

## Abstract

The monogonont rotifer *Bryceella stylata* was investigated with light, electron and confocal laser scanning (CLSM) microscopy to provide detailed insights into its anatomy and new information for future phylogenetic analyses of the group. Results from CLSM and phalloidin staining revealed a total of six paired longitudinal muscles (musculi longitudinales I–VI) and eight circular muscles (musculi circulares I–VIII) as well as a complex network of mostly fine visceral muscles. In comparison with other rotifer species that have been investigated so far, *B. stylata* shares the presence of the circular and longitudinal muscles: musculus longitudinalis ventralis, musculus longitudinalis lateralis inferior, musculus longitudinalis dorsalis, musculus longitudinalis capitis and musculus circumpedalis. However, the species lacks lateral and dorsolateral longitudinal muscles and some circular muscles (e.g., corona sphincter, musculus pars coronalis). With light and electron microscopy, we were able to document the precise number of pseudosegments and the arrangement of the chambers comprising the trophi elements. Furthermore, our observations revealed several new morphological characteristics, including a shield-like epidermal projection covering the dorsal antenna, an epidermal projection restricting the corona caudally and an unpaired hypopharynx with distinct shovel-like structures. © 2009 Elsevier GmbH. All rights reserved.

**Keywords:** Rotifera; Proalidae; Morphology; Musculature; Confocal laser scanning microscopy

---

## 1. Introduction

Our knowledge of the rotiferan musculature has improved recently in large measure due to the application of phalloidin-labelled dye combined with confocal laser scanning microscopy (CLSM) (e.g., Hochberg and Litvaitis 2000; Sørensen et al. 2003; Sørensen 2005a,

2005b; Kotikova et al. 2006; Riemann et al. 2009). But these and other similar papers still investigate only a small fraction of rotiferan taxa. A broader overview of the complex rotifer muscular system can only be achieved on the basis of adequate taxon sampling by including as many genera as possible. Data from further taxa are essential to accumulate more information about morphological variation in rotifer musculature and to retrace its evolution in detail (as emphasized by Sørensen 2005a; Kotikova et al. 2001).

---

\*Corresponding author.

E-mail address: [eike.f.wilts@mail.uni-oldenburg.de](mailto:eike.f.wilts@mail.uni-oldenburg.de) (E.F. Wilts).

The aim of this study is to contribute new data about rotiferan musculature in general and species of Proalidae in particular. Within Proalidae, detailed descriptions of the somatic musculature patterns exist for only a few species of *Proales* Gosse, 1886. As a first step towards addressing this deficiency, we provide the first description of the somatic musculature in a species of *Bryceella* using CLSM techniques. For small-sized species such as this, CLSM has proven itself to be a very potent technique to visualize even the finest fibres that are otherwise difficult to observe in detail using conventional light microscopy.

Although the small, dorsoventrally flattened species of *Bryceella* are common in different aquatic and semiaquatic habitats (e.g., moors, the psammon of acid waters, ponds, mosses and leaf litter), our knowledge of their morphology remains fragmentary. We found the cosmopolitan rotifer *Bryceella stylata* (Milne, 1886) in mosses from a forest in Leer, North-west Germany and seized the opportunity to reinvestigate its internal and external morphology using light and electron microscopic techniques. Facing the lack of available appropriate morphological investigations across Proalidae and the necessity of a revision of this non-monophyletic group (see Wilts et al. 2009), our goal is to improve existing descriptions of this species and to present new morphological details to support a subsequent phylogenetic analysis that will hopefully clarify both the phylogenetic position of *Bryceella* and the phylogeny of Proalidae in general.

## 2. Material and methods

Moist mosses were collected during January 2007 from a forest in Leer, North-west Germany (53°15'48.14"N, 7°31'54.46"E), transported to the laboratory and subsequently cultured in plastic bags over several weeks.

Single rotifer specimens were studied by both differential interference light microscopy (Leica DMLB) and electron microscopy. Light microscopic images were taken with a digital camera (Olympus ColorView). Isolated rotifer specimens were narcotized with bupivacaine (Bucain®) and fixed with a 4% OsO<sub>4</sub> solution and picric acid formaldehyde at 240 mOsm (after Melone 1998). Specimens were dehydrated in a graded ethanol series followed by critical-point drying. Dried specimens were mounted on stubs and coated with gold. Trophi were prepared under a stereomicroscope (Leica MZ12<sub>5</sub>) following the procedure of De Smet (1998) but using SDS/DTT (modified after Kleinow et al. 1990) as the dissolving agent. Specimens and trophi were studied by scanning electron microscopy (SEM; Zeiss DSM 940).

For transmission electron microscopic (TEM) studies, specimens were immobilized by exposing them to an aqueous solution of 0.25% bupivacaine for 1 min and subsequently fixing them with 1% OsO<sub>4</sub> in 0.1 M sodium cacodylate buffer at 8 °C. After fixation, specimens were dehydrated in an increasing acetone series at 8 °C, subsequently embedded in Araldite hardened at 60 °C for 72 h and ultrasectioned (75 nm) on a Reichert ultracut followed by automatic staining with uranyl acetate and lead citrate (Leica EM Stain). Examination of the ultrathin sections was performed on a Zeiss 902 TEM at 80 kV.

For CLSM, specimens were placed in a drop of freshwater and relaxed in a 0.25% solution of bupivacaine at 8 °C. The anaesthetised specimens were fixed for 1 h in phosphate-buffered 4% paraformaldehyde and rinsed in 0.1 M phosphate-buffered saline (PBS), and then made permeable for staining by exposure to 0.1% Triton X-100 buffered in 0.1 M PBS for 1 h. For staining, 2 µl of 38 µM methanolic TRITC-labelled phalloidin solution were added to 100 µl of Triton X-100 buffered in 0.1 M PBS. Specimens were stained for 3 h and mounted in Citifluor® on a cover slip; a total of five specimens were analyzed. The images were obtained under wavelength of 488 nm using a Leica TCS SP 5 confocal laser scanning microscope. We used ImageJ 1.37v and Leica LAS AF 1.7.0 for analysis of the image stacks. Line drawings were prepared using Adobe Photoshop® CS2.

Our descriptions of the individual mastax jaw elements (trophi) and their relative positions follow the terminology previously introduced by Riemann et al. (2009), except that the terms *dorsal manubrial chamber opening*, *median manubrial chamber opening* and *ventral manubrial chamber opening* are replaced by *manubrium foramen dorsalis*, *manubrium foramen medius* and *manubrium foramen ventralis* in this study.

## 3. Results

### 3.1. Diagnosis

Small, dorsoventrally flattened body; head region narrow, trunk bulbous, foot slender; corona with two long lateral styli and forward directed cirri; rostrum oval and broad; foot with three pseudosegments and inwardly curving toes, consisting of three articulating joints; rami with six delicate spine-shaped projections anteriorly; distal subuncus with denticulate margin beneath the unci; fulcrum caudally slanted with ventrally directed hook; manubria broad, tapering distally; multilayered hypopharynx with a paired shovel-like structure anteriorly.

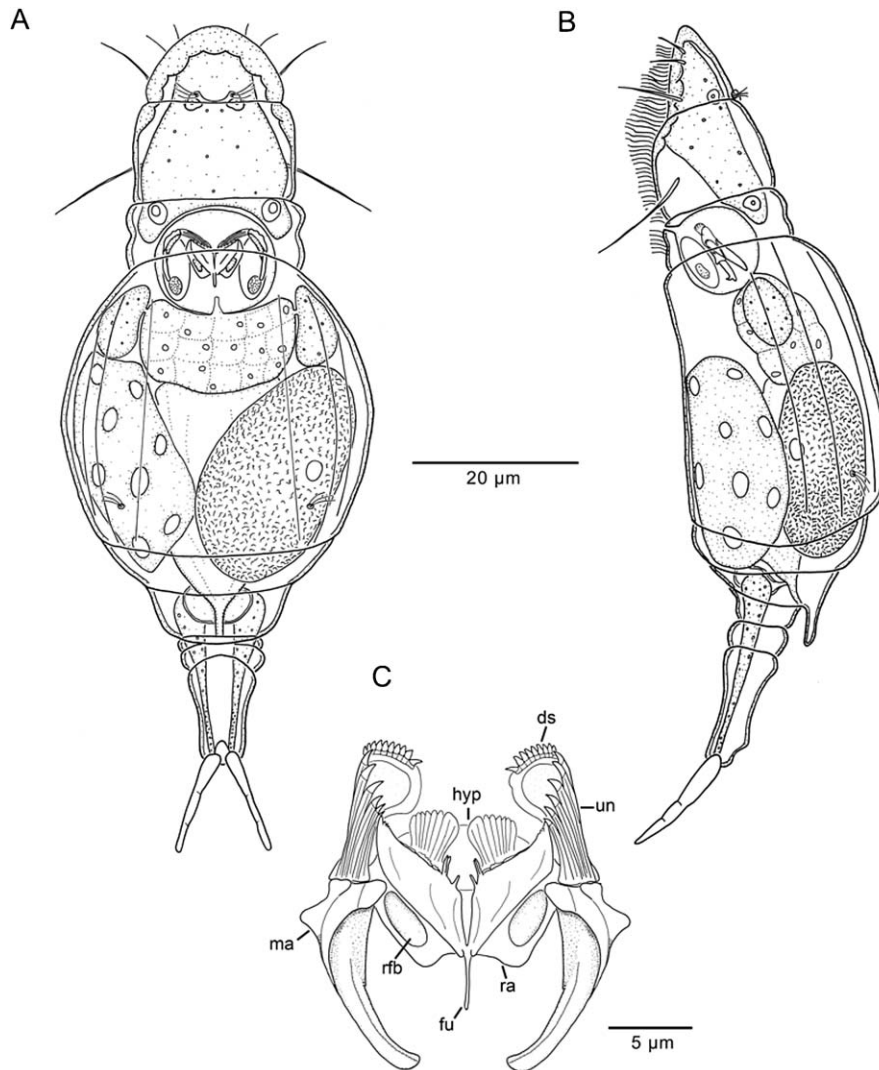


**Fig. 1.** General body organization of *Bryceella stylata*. (A) Specimen from dorsal side; (B) specimen in lateral view; (C) mastax hard parts (trophi) in dorsal view. ds = distal subuncus, fu = fulcrum, hyp = hypopharynx, ma = manubrium, ra = ramus, un = uncus.

### 3.2. General body organization of parthenogenetic females

#### 3.2.1. Habitus

*B. stylata* has a hyaline and weakly stiffened, dorsoventrally flattened body with a narrow head, a bulbous trunk and a slender foot (Figs. 1A and 2A). The whole body is divided into three distinct regions: head with neck, trunk and foot with toes (Figs. 1A, B and 3A, B). The surface of the epidermis is smooth. TEM sections reveal a syncytial postcoronal integument with a thin intrasyncytial layer of electron-dense material that shows deep, bulb-like invaginations of the plasmalemma at more or less continuous intervals.

The head is only partly contractible into the trunk and is divided into three pseudosegments separated from each other and the trunk by distinct transverse folds

(Fig. 3B). The most anterior pseudosegment presents a large, semicircular to oval rostrum (Fig. 2B) and is followed by two additional short and rectangular pseudosegments (Figs. 1B and 3C, D) in which the trophi (Fig. 2A, C, D) are located. A dorsal antenna inserts at the intersection of the first and second head pseudosegments (Fig. 3D). The third head pseudosegment, the so-called neck pseudosegment, adjoins the trunk. The planar corona is limited to the ventral head region and extends ventrally from the most anterior pseudosegment to the neck pseudosegment, where a small epidermal projection restricts it caudally (Fig. 3A, C). The corona (Fig. 2A, E) presents several long anteriorly directed cirri (stuck cilia) and a pair of long laterally directed cirri, the so-called styli (Figs. 1A, 2A and 4A). SEM images and different TEM sections reveal that the styli are composed of about 14 cilia (Fig. 4B). One large pair of light-refracting bodies exists laterally

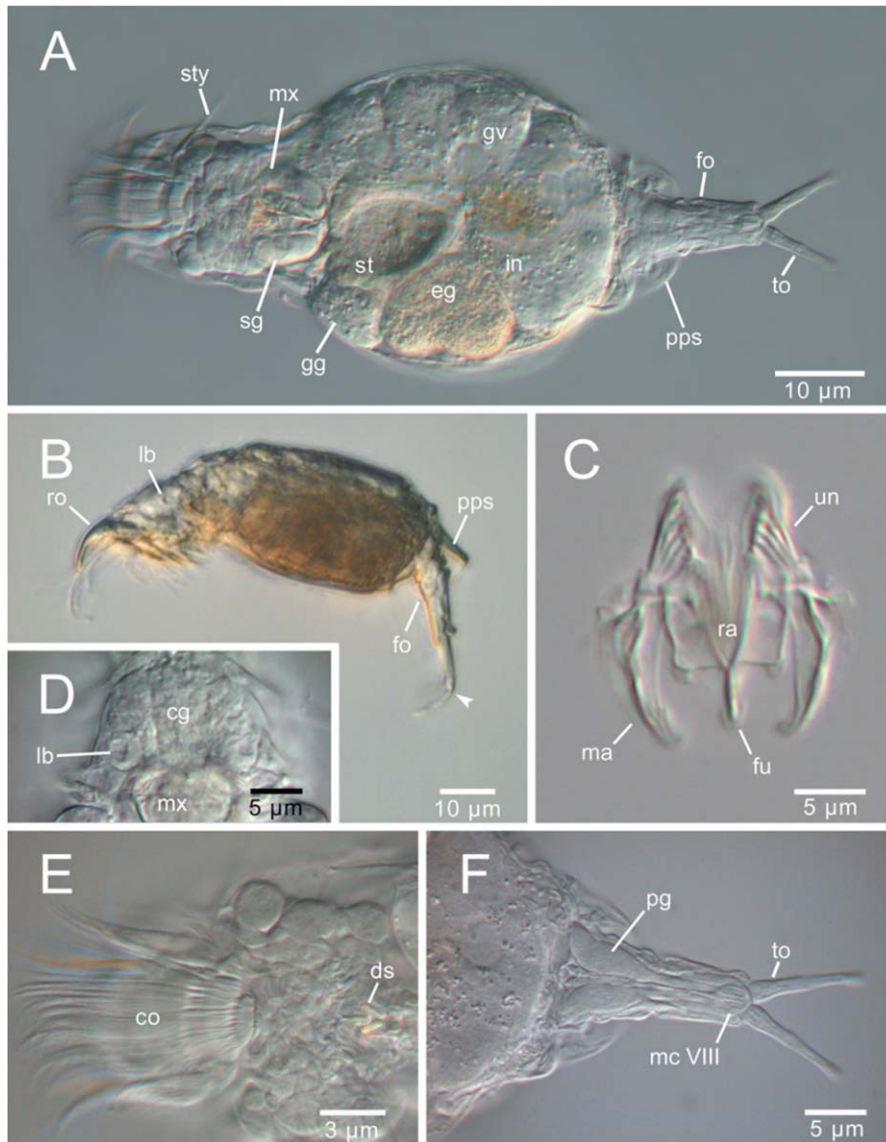


**Fig. 2.** Light microscopic images of *Bryceella stylata*. (A) Adult specimen in ventral view; (B) specimen in lateral view; (C) mastax hard parts (trophi); (D) head with light refracting bodies in front of the mastax; (E) head with corona; (F) foot. cg = cerebral ganglion, co = corona, ds = distal subuncus, eg = egg, fo = foot, fu = fulcrum, gg = gastric gland, gv = germovitellarium, in = intestine, lb = light refracting body, ma = manubrium, mc VIII = musculus circumpedalis, mx = mastax, pg = pedal gland, pps = preanal pseudosegment, ra = ramus, ro = rostrum, sg = salivary gland, st = stomach, sty = stylus, to = toe, un = uncus. Arrow head (ventral breaks of articulating joints).

in the head near the styli. Several other light-refracting bodies are scattered throughout the head (Figs. 2D and 4C).

The ovoid trunk is wider than the head and is also divided into three pseudosegments that are again separated by distinct transverse folds. The anteriormost and largest pseudosegment bears the lateral antennae posteriorly and presents four longitudinal ridges separated by three longitudinal folds (Fig. 3B). The anteriormost pseudosegment is followed by a shorter and narrower lumbar pseudosegment. The third semicircular

preanal pseudosegment overlaps the foot partially (Figs. 1B, 2B and 3A).

The slender foot tapers conically and is divided into one long terminal segment followed by two shorter basal ones (Fig. 1A) and two long, rod-shaped toes, characterized by two ventral constrictions (Figs. 1B and 3A). The toes are partially retractable into the caudalmost foot pseudosegment and terminate in rounded tips. Viewed dorsally, the toes are normally spread (Fig. 2F). During swimming, the foot is directed somewhat ventrally; otherwise, it is caudally directed. Two pedal



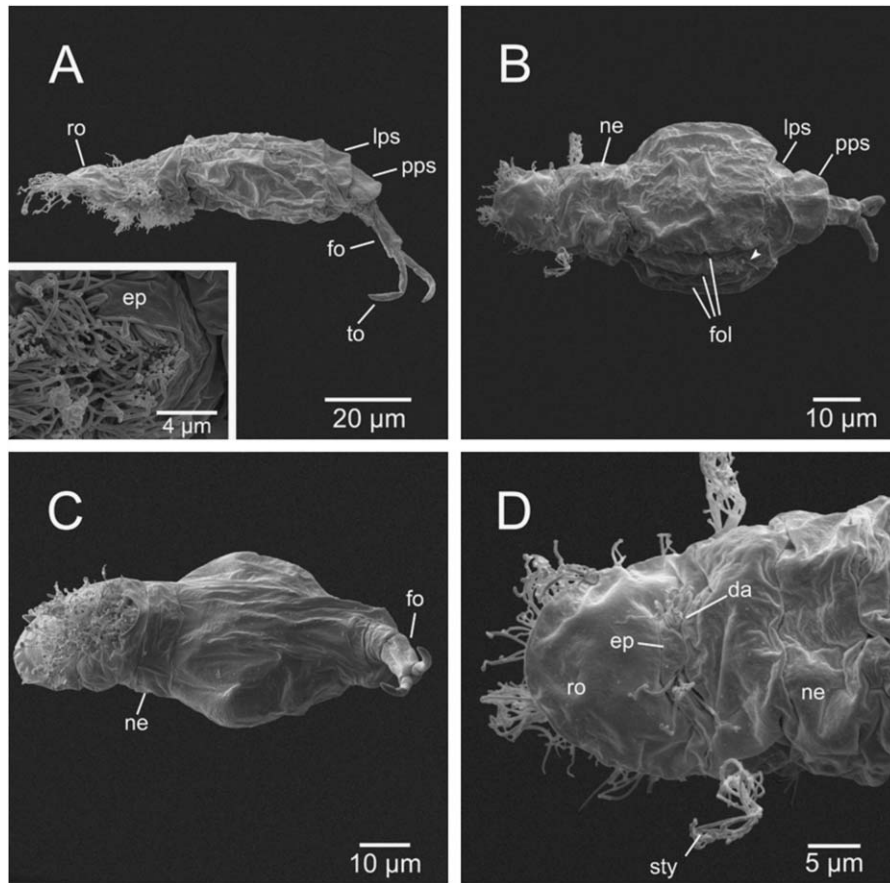


**Fig. 3.** Scanning electron microscopic (SEM) images of *Bryceella stylata*. (A) Specimen in lateral view (detail: ventral view of epidermal projection restricting the corona caudally); (B) specimen in dorsal view; (C) specimen in ventral view; (D) head in dorsal view. da = dorsal antenna, ep = epidermal projection, fo = foot, fol = longitudinal folds, lps = lumbar pseudo-segment, ne = neck, pps = preanal pseudo-segment, ro = rostrum, sty = stylus, to = toe. Arrow head (position of lateral antenna).

glands extend through the foot and broaden in the basal foot pseudo-segment (Fig. 2F).

### 3.2.2. Digestive system

The digestive tract consists of the mouth opening, the spherical mastax, the narrow oesophagus, the stomach and the intestine (Figs. 1A, B and 2A). The mouth opening is located ventrally in the center of the neck pseudo-segment and leads to a short buccal tube and the mastax cavity. The mastax is located at level of the transverse fold dividing the neck and the trunk (Figs. 1A and 2A). A pair of salivary glands is visible laterally in the mastax complex (Fig. 2A). The oesophagus diverges dorsally from the mastax and leads to the relatively small stomach situated in the first trunk pseudo-segment. A pair of bulbous gastric glands diverges anteriorly from the stomach wall (Fig. 2A). The stomach and the intestine are separated by a constriction. The ciliated intestine leads to the cloaca that opens dorsally below the preanal pseudo-segment.

3.2.2.1. Mastax hard parts (trophi). The trophi are generally bilateral symmetrical, although they show minor asymmetry (Figs. 1C and 5A).

The unpaired fulcrum usually resides in the longitudinal axis of the body and attaches obliquely to the rami with its terminal end directed caudally. In ventral view it appears slender and rod-shaped and presents an oval apophysis at its base (Fig. 5B); in lateral view, it shows an extension and a slanted distal end with a ventrally directed hook (Fig. 5C).

The individual ramus basal chambers are triangular and appear rhombic in combination when observed dorsally. Each ramus is serrated anteriorly with several minor and three long, spinous projections formed by the ramus subbasal chamber. Two of these latter projections lie closely together, with the remaining one being more isolated (Fig. 5A). Posteriorly, the ramus subbasal chambers are rounded and alulae are lacking. Both the ramus basal and the ramus subbasal chamber display distinct openings with the large widened, quadrangular ramus foramen subbasalis directed ventrally (Fig. 5B)

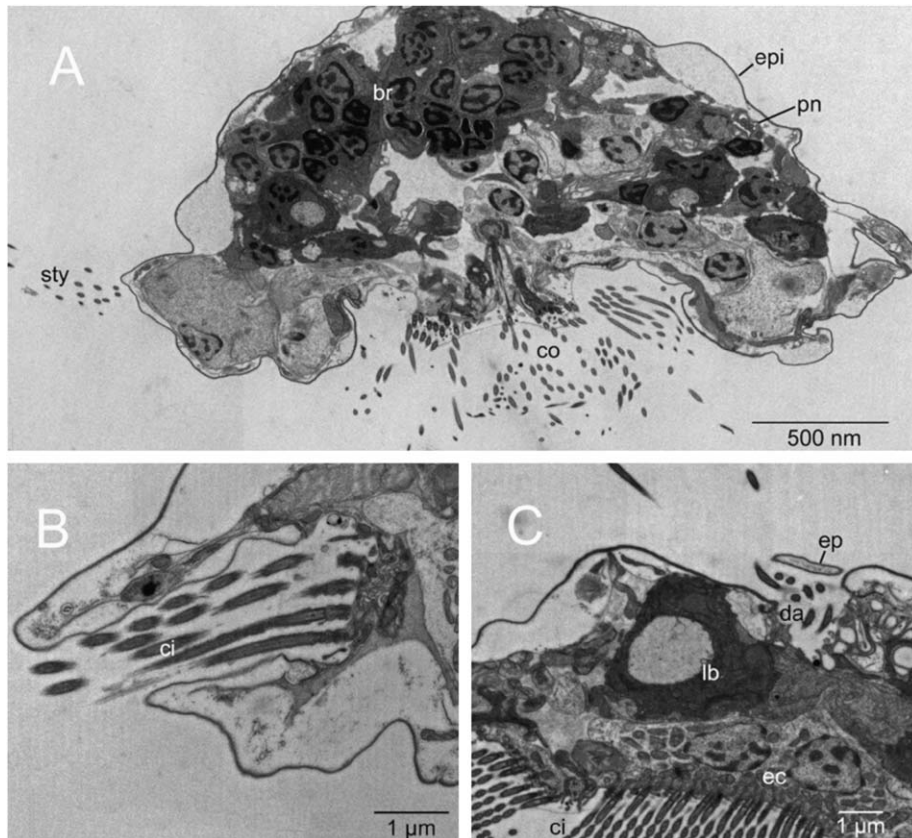


**Fig. 4.** Transmission electron microscopic (TEM) images of cross sections of the head of *Bryceella stylata*. (A) Overview of posterior region; (B) section through stylus (note the ventrolateral position apart from the rest of the corona); (C) Detail of the middle head region. br = brain, ci = cilia, co = corona, da = dorsal antenna, ec = epidermal cushioning, ep = epidermal projection, epi = epidermis, lb = light refracting body, pn = protonephridium, sty = stylus.

and the large, rounded ramus foramen basalis facing dorsally (Fig. 5A, D, E). An unpaired, hypopharynx with two digitated, laminar, shovel-shaped planes anteriorly is located ventral to the rami (Figs. 1C, 2C and 5A, D, F).

The paired unci are built on domed plates, each carrying six unci teeth decreasing gradually in length from dorsal- to the ventralmost tooth. Beneath each of these bent principal teeth lies a smaller accessory, angular toothlet. A large and lobate distal subuncus is located ventral to the uncus. It presents about nine denticles that seem to follow the row of the unci teeth (Fig. 5A, F). In live specimens, the small denticles of the distal subuncus are in close contact with the anterior margin of the ventral surface of the rami.

The sickle-shaped manubria attach to the unci proximally by fine ligaments and taper gradually from the broad clava towards the end of the inwardly curved cauda (Fig. 5A, B). The three manubrial chambers represent cuticular pockets with lamellar walls and distinct openings (foramina) (Fig. 5A). In *B. stylata*, these walls are almost completely dispersed and are only

recognizable as small ridges that are best seen in lateral and caudal views on SEM images (Fig. 5C, E). Whereas the median and the dorsal manubrial chambers form the cauda, the ventral manubrial chamber is smaller and accounts for only one-third of the manubrial length. The manubrium foramen ventralis is ventrally directed (Fig. 5B). The manubrium foramen medius and the manubrium foramen dorsalis extend completely to the end of the cauda (Fig. 5E). In caudal view, the lamellar wall separating these two foramina is visible as a fine ridge in the posterior part of the cauda.

### 3.2.3. Nervous system and sensory organs

The occipital cerebral ganglion is situated in the anterior part of the head in front of the mastax (Figs. 1A, 2D and 4A). The dorsal antenna is located on the head directly behind the rostrum. A shield-like projection of the epidermis arches frontally upwards and backwards over the dorsal antenna caudally from where cilia protrude under the projection on both sides (Figs. 3D and 4C). The lateral antennae consist of a few cilia with a flat, rounded collar and are located in the

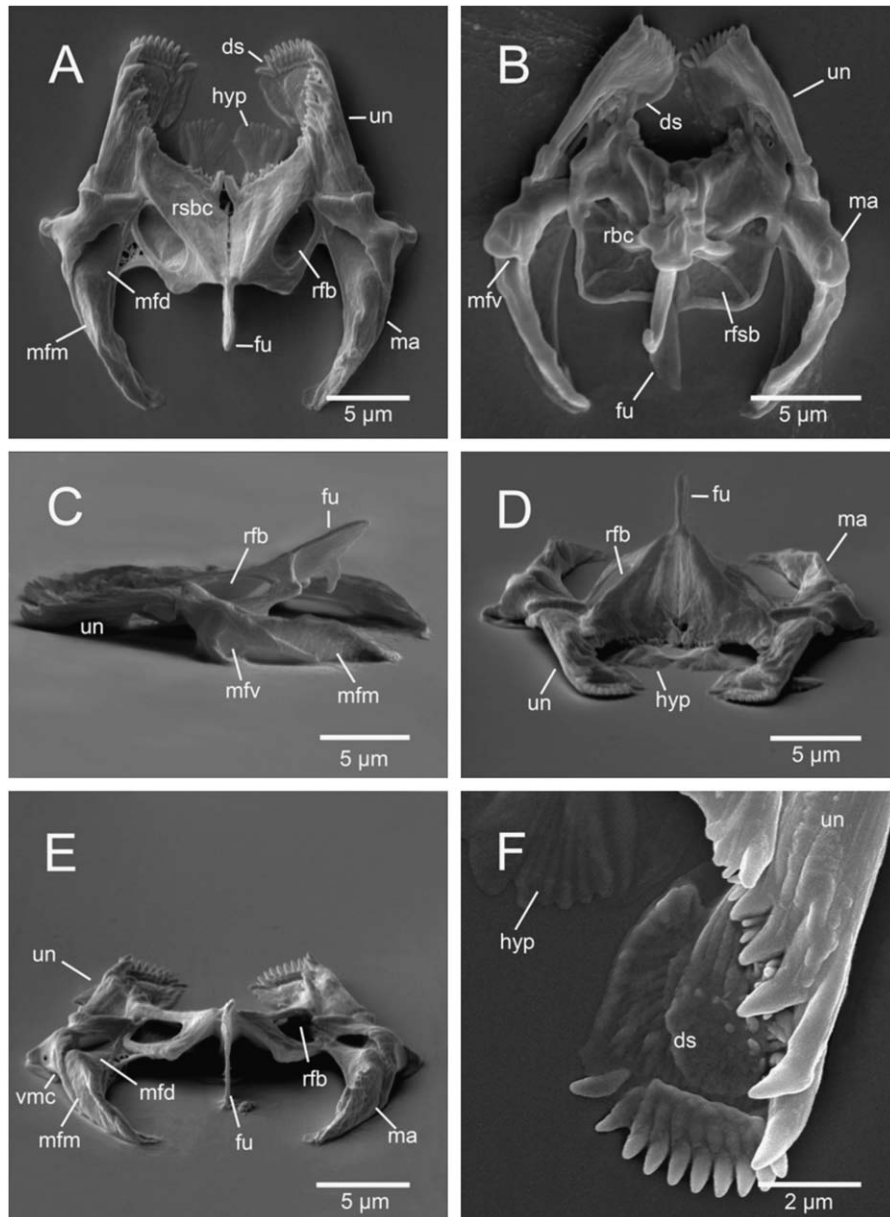


**Fig. 5.** Scanning electron microscopic (SEM) images of the mastax hard parts (trophi). (A) Trophi in dorsal view; (B) trophi in ventral view; (C) trophi in lateral view; (D) trophi in dorsofrontal view; (E) trophi in dorsocaudal view; (F) uncus with distal subuncus. ds=distal subuncus, fu=fulcrum, hyp=hypopharynx, ma=manubrium, mfd=manubrium foramen dorsalis, mfm=manubrium foramen medius, mfv=manubrium foramen ventralis, rbc=ramus basal chamber, rfb=ramus foramen basalis, rfsb=ramus foramen subbasalis, rsbc=ramus subbasal chamber, un=uncus, vmc=ventral manubrial chamber.

last third of the anteriormost trunk pseudosegment (Fig. 3B).

#### 3.2.4. Excretory system

The protonephridial system consists of four serial pairs of distinct terminal organs (Fig. 4A) distributed laterally in the body cavity, along the longitudinal axis of the animal. The collecting tubules open into a contractile bladder that is positioned ventrocaudally in

the trunk. The fluid of the bladder is emptied into the terminal part of the intestine (cloaca).

#### 3.2.5. Reproductive organs

*B. stylata* is an oviparous species. The parthenogenetic females possess a syncytial germovitelarium situated dorsolaterally in the posterior part of the trunk. The vitellarium contains eight nuclei (Figs. 1B and 2A).

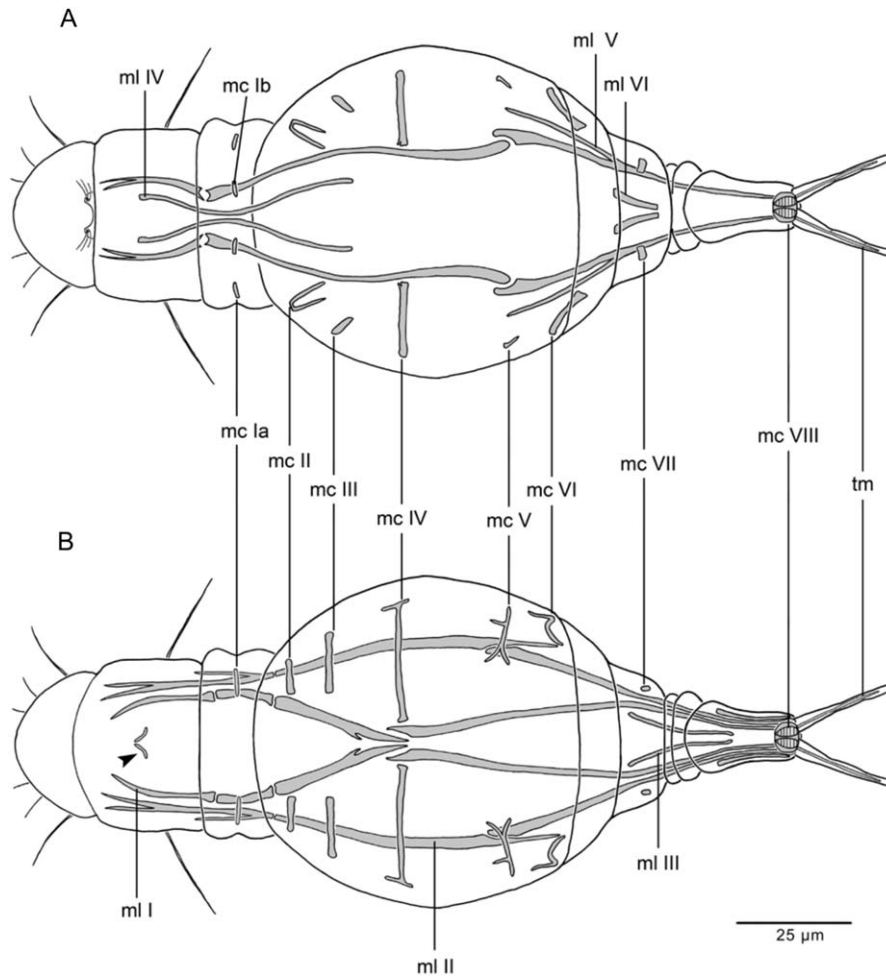


**Fig. 6.** Schematic drawing of the somatic musculature of *Bryceella stylata*. (A) Dorsal view; (B) ventral view. mc Ia–VIII = musculi circulares Ia–VIII, ml I–VI = musculi longitudinales I–VI, tm = toe muscle.

Most of the observed amictic females possessed one large, ovoid egg.

### 3.2.6. Measurements

Total length 90–180 μm, maximum dorsoventral dimension 22 μm, maximum width 35–54 μm, foot length 31–42 μm, toe length 16–20 μm, trophi length 23 μm, trophi width 18 μm, ramus length 10 μm, manubria length 13 μm, cauda width 6 μm and fulcrum length 4 μm.

## 3.3. Somatic musculature

### 3.3.1. Longitudinal muscles

In *B. stylata*, the somatic muscular system consists of six pairs of longitudinal muscles (musculus longitudinalis I–VI). Musculus longitudinalis I, II and V span the distance from the head to the toes, whereas the remaining longitudinal muscles are significantly shorter.

The longitudinal muscles differ in number of their subunits with musculus longitudinalis I consisting of four subunits, musculus longitudinalis III, IV and VI of one subunit only, musculus longitudinalis II of two, and musculus longitudinalis V of three subunits (Fig. 6A, B).

Musculus longitudinalis I (m. longitudinalis ventralis) is the ventralmost pair of longitudinal muscles, running from the head to the base of the toes. Each strand broadens in the middle of its length. This, together with the convergent courses of the muscle strands, causes the two muscles to form an x-shape medially in the trunk (Figs. 6B and 7A, B).

The paired musculus longitudinalis II (m. longitudinalis lateralis inferior) (Figs. 6A and 7B) extends from the head to the base of the toes ventrolaterally. Each of the two muscle strands consists of two subunits. The anterior subunit splits further in the anteriormost region of the trunk. One branch terminates in the neck pseudosegment, with the second bifurcating anteriorly



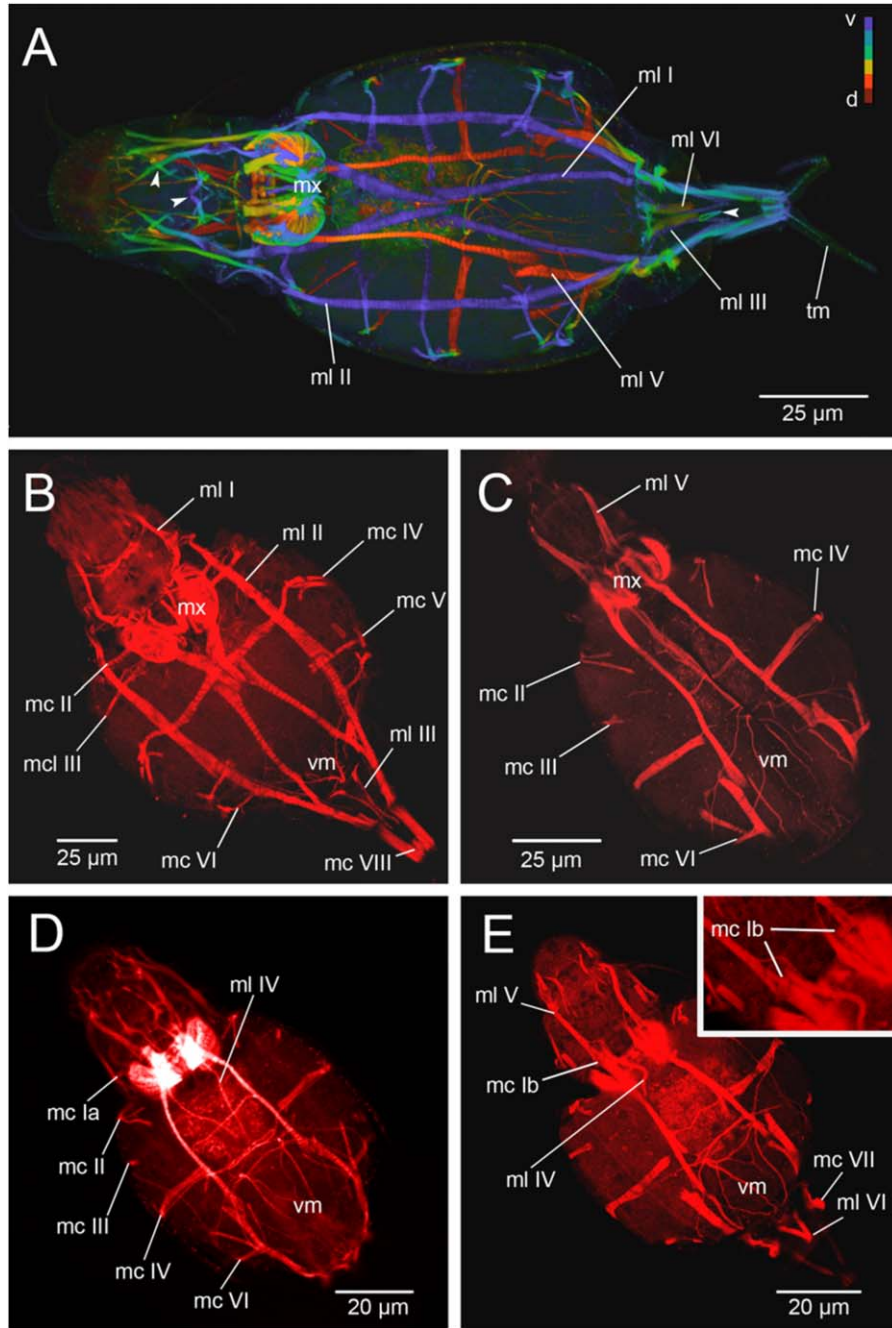


**Fig. 7.** Somatic musculature of *Bryceella stylata*. Fluorescent phalloidin-staining of f-actin filaments, confocal laser scanning microscopy (CLSM). (A) Depth-coded maximum projection of fluorescence signals (specimen 1); (B) fluorescence signals of ventral body region (specimen 2); (C) fluorescence signals of dorsal body region (specimen 1); (D) fluorescence signals of dorsal body region (specimen 3); (E) fluorescence signals of dorsal body region (specimen 2) (detail: closer view of musculus circularis b). mc Ia–VIII = musculi circulares Ia–VIII, ml I–VI = musculi longitudinales I–VI, mx = mastax, tm = toe muscle, vm = visceral musculature. Arrow heads (unidentified muscles).

in the head (Fig. 6B). In the caudalmost foot pseudosegment, the muscles show a lateral enlargement following the main strands to the toes (Figs. 6B and 7A, B).

The two muscles of the short and slender paired musculus longitudinalis III stretch ventrally from the

preanal pseudosegment to the middle of the terminal foot pseudosegment (Figs. 6B and 7A, B).

The slender, paired musculus longitudinalis IV (m. longitudinalis capitis) runs dorsally from the head to the anteriormost third of the trunk. This muscle pair

was not easily visualized in all the examined specimens (Figs. 6A and 7D, E).

Musculus longitudinalis V (m. longitudinalis dorsalis) stretches along the dorsalmost part of the animal, extending from a point behind the rostrum to the base of the toes. The third subunit in each muscle presents a long, fine apically stretching strand (Figs. 6A and 7A, C–E).

The short, paired musculus longitudinalis VI is attached to the caudal end of the preanal pseudosegment and terminates at the transition of the lumbar pseudosegment (Figs. 6A and 7A, E). The muscle is broad, but without any recognizable cross-striation.

### 3.3.2. Circular muscles

A total of eight circular muscles (musculi circulares I–VIII) were identified. Except for musculus circularis VIII, all circular muscles are interrupted both dorsally and ventrally and otherwise show various degrees of incompleteness.

Musculus circularis I is a very fine, incomplete muscle in the neck region, recognizable as short, narrow ventrolateral (musculus circularis Ia) and dorsal bands (musculus circularis Ib) that are completely disconnected from one another (Figs. 6A, B and 7D, E).

Musculus circularis II is positioned in the trunk directly behind the neck. Ventrally it broadens and reaches to the level of the mastax; dorsally it splits into two fine fibres, each directed slightly caudally (Figs. 6A, B and 7A–D).

Musculus circularis III is situated in the foremost third of the trunk. It is incomplete and ventrolaterally displaced (Figs. 6A, B and 7C, D).

Musculus circularis IV is positioned near the midpoint of the longitudinal body axis. Ventrally, the muscle virtually reaches the midline of the body. Dorsally, the muscle becomes increasingly robust and reaches the level of musculus longitudinalis V. Ventrolateral the muscle splits up irregularly (Figs. 6A, B and 7B–D).

Musculus circularis V is located in the posteriormost third of the trunk. Ventrally, the muscle bifurcates at the level of the musculus longitudinalis II and terminates dorsolaterally (Figs. 6A, B and 7A, B).

Musculus circularis VI follows directly posterior to musculus circularis V. Like musculus circularis V, it also bifurcates ventrally, with one branch arising close to the fine caudally stretching strand of the second subunit of musculus longitudinalis II. Dorsally, the muscle reaches to the apically stretching branch of the caudalmost subunit of musculus longitudinalis V (Figs. 6A, B and 7B–D).

Musculus circularis VII is located in the preanal pseudosegment and expands laterally (Figs. 6A, B and 7A, E) to envelope the musculus longitudinalis V.

Unlike the remaining circular muscles, musculus circularis VIII (m. circumpedalis) forms a complete ring in the caudalmost region of the last foot pseudosegment in front of the bases of the toes. It is composed of three distinct strands (two laterally and one in the midline) connected by a complex bundle of very fine fibres. This complex is connected to a pair of cross-striated muscles that stretches through the toes (Figs. 2F, 6A, B and 7A, B).

### 3.3.3. Visceral musculature

*B. stylata* presents a complex network of visceral musculature characterized by fine circular, longitudinal and transverse visceral muscles encircling parts of the digestive system including the stomach, gut and bladder. Anteriorly, the muscles of the digestive system comprise one incomplete circular fibre and numerous other fibres. Additionally, two complete circular and numerous longitudinal fibres were identified posteriorly. However, some of these fibres change their course in a transverse direction (Fig. 7C–E). Furthermore, although a fine network of muscles is associated with the bladder in the posterior part of the body, it is too complex and stains too weakly to be examined and described in any detail here. The mastax musculature gives an intense fluorescence signal. It comprises a number of strong, distinctly cross-striated muscles (Fig. 7A–C). Several other actin-containing fibres with a morphology and/or orientation differing from the typical circular and longitudinal muscles were also apparent, largely in the head region, but could not be classified because of their unusual course and unknown function. These muscles are not considered in the reconstructions, but are clearly visible in all analyzed specimens (arrow heads Fig. 7A). One of these muscles is paired and located in the anterior head region, crossing diagonally forward from ventral to dorsal above the anterior end of the musculus longitudinalis ventralis (m. longitudinalis I). A second unidentified muscle is short, paired and located in the center of the head. Its two subunits are closely associated ventrally before diverging laterally. A third muscle consists of a plane of ringlike muscle that is located in the terminal foot pseudosegment.

## 3.4. Ecology and behaviour

*B. stylata* seems to occur more frequently in colder seasons and infrequently during warm periods. Due to the heat development on the glass slide or in the Petri dish induced by the microscope light, specimens often roll on their dorsal side and contract. Specimens swim in the water column with their head and foot directed somewhat ventrally. Usually they glide in a nimbly or jerky manner on the ground or graze on detritus particles. Specimens were often observed swimming on

their dorsal side, rolling a detritus-ball with their corona.

## 4. Discussion

### 4.1. Somatic musculature within *B. stylata* and across Rotifera

The somatic musculature in five specimens was visualized by CLSM. All specimens were examined in dorsoventral position, because their dorsoventral flatness precluding a lateral observation. A comparison of the image stacks showed that examining multiple specimens is absolutely necessary for a successful reconstruction because all muscles often could not be recognized in each specimen. The somatic muscle system in *B. stylata* comprises longitudinal and circular muscles that are paired, bilateral and symmetrical. The circular muscles directly underlie the integument and are inwardly followed by the longitudinal muscles. All muscles, including the circular ones, show a conspicuous pattern of cross-striation.

Hitherto, no detailed information on the musculature of a *Bryceella* species exists, although, to our surprise, Milne (1886) already observed a ventral muscle pair in *B. stylata* that he attributed to stretching and relaxing of the trunk. In the context of the present paper, this pair is likely to be musculus longitudinalis I. Our CLSM-analyses of the stained whole-mount specimens filled this gap to reveal substantial new information on the musculature of *B. stylata*, thereby improving our knowledge of the muscular system within Proalidae. In the following discussion we attempt to characterize the function of these newly described muscles in *B. stylata* and homologize them with muscles in other species of Rotifera described using similar methods.

In *B. stylata*, the somatic muscular system comprises complete and incomplete circular and longitudinal muscles, the latter lying internal to the former. This muscle arrangement is present in all rotifers examined to date, with dorsal, lateral and ventral retractors as well as incomplete circular muscles having been considered to be a basal trait in this group of aquatic invertebrates (see Hochberg and Litvaitis 2000; Santo et al. 2005; Sørensen 2005a; Riemann et al. 2008). The longitudinal muscles act as retractors on the head and the foot; the circular muscles, working against the hydrostatic pressure of the pseudocoelom, produce a transverse contraction and an elongation of the body (Santo et al. 2005). Although different in detail, the system of circular and longitudinal muscles is assumed to be homologous across all rotifer species.

Paired musculi longitudinales ventrales have been detected in several monogonont genera including

*Synchaeta* (musculus retractor ventralis, see Peters 1931); *Notommata*, *Floscularia* and *Brachionus* (ventral retractor of corona, see Santo et al. 2005); *Proales* (ventral trunk retractors, see Sørensen 2005a); *Dicranophorus* and *Encentrum* (musculus longitudinalis ventralis, see Riemann et al. 2008) and *Beauchampiella* (musculus longitudinalis ventralis, see Riemann et al. 2009). In the bdelloid taxon *Philodina*, Hochberg and Litvaitis (2000) found a single ventral pair of longitudinal muscles spanning the length of the individual. In *B. stylata*, the musculi longitudinales ventrales (musculus longitudinalis I) likewise span the length of the body, converging in the middle of the trunk, attaching caudally to the musculus circumpedalis in front of the toes. This presence of a pair of ventral longitudinal muscles in *Bryceella* has to be considered plesiomorphic based on the argument by Riemann et al. (2008) that a pair of uninterrupted ventral longitudinal muscles is a ground pattern feature of Rotifera.

The presence of paired ventrolateral muscles is shared by numerous rotifer species such as *Conochilus natans* (musculus retractor lateralis inferior, see Remane 1929–1933; Hlava 1905); *Epiphanes senta* (musculus retractor lateralis inferior, see Remane 1929–1933; Martini 1912); *Rhinoglena crystallina* (musculus retractor lateralis inferior, see Stoßberg 1932); *Proales reinhardti* and *Proales daphnicola* (ventrolateral trunk retractors, see Sørensen 2005a); *Testudinella patina* (ventrolateral corona retractor, see Sørensen 2005b); *Filinia novaezealandiae* (ventrolateral retractor, see Hochberg and Gurbuz 2007); *Encentrum mucronatum* (musculus longitudinalis II, see Riemann et al. 2008). *B. stylata* similarly features a ventrolateral muscle pair (musculus longitudinalis II) anchoring bifurcate behind the rostrum and extending to the base of the toes. However, this muscle is relatively longer than that in most of the investigated species. The exception includes *C. natans*, where the ventrolateral muscle pair traverses the whole animal and *P. daphnicola*, where the ventrolateral muscles run from the head almost to the tip of the toes. By contrast, in *P. reinhardti*, *R. crystallina*, *E. mucronatum* and *E. senta*, the ventrolateral muscles start in the head and terminate in the caudal region of the trunk. In *D. forcipatus*, the muscles stretch from the neck to the caudal end of the trunk. The ventrolateral muscle pair in *F. novaezealandiae* and *T. patina* only reaches from the head to the middle of the trunk. Even so, given its distribution throughout Ploima and Gnesiotrocha, we consider the ventrolateral muscle pair to be homologous and call them musculi longitudinales laterales inferior (sg. musculus longitudinalis lateralis inferior). Moreover, due to its wide distribution, we assume this muscle pair to be a ground pattern feature of Monogononta; the data for Bdelloidea are ambiguous at the moment.



Hence for *B. stylata*, the ventrolateral muscle pair would appear to be a plesiomorphic trait.

A dorsal longitudinal muscle pair has been detected in several monogonont and bdelloid rotifer species including *C. natans* and *Lindia tecusa* (musculus retractor dorsalis, see Remane 1929–33); *Mniobia symbiotica* (dorsaler Längsmuskel, see Remane 1929–1933); *Synchaeta baltica* (musculus retractor dorsalis, see Peters 1931); *Notholca acuminata* (dorsal retractor, see Sørensen et al. 2003); *Brachionus urceolaris* and *Floscularia ringens* (dorsal retractor muscle, see Santo et al. 2005); *P. reinhardti*, *P. fallaciosa* and *P. daphnicola* (dorsal trunk retractor, see Sørensen 2005a); *Philodina* sp. (longitudinal bands, see Hochberg and Litvaitis 2000); *Dicranophorus forcipatus*, and *E. mucronatum* (musculus longitudinalis dorsalis, see Riemann et al. 2008); *Beauchampiella eudactylota* (musculus longitudinalis dorsalis, see Riemann et al. 2009). In *P. reinhardti*, *P. fallaciosa*, *Philodina* sp., *C. natans*, *F. ringens*, *D. forcipatus* and *E. mucronatum*, the muscle stretches along the whole body from the head to the foot. In *L. tecusa*, it originates behind the head and extends to the foot. In *M. symbiotica*, it also starts behind the head, but terminates in the caudal trunk region. In *B. eudactylota* and *S. baltica*, the dorsal muscle pair extends from the head up to the caudal region of the trunk. It is even shorter in *P. daphnicola*, *N. acuminata* and *B. urceolaris*, in which the muscles start in the head and terminate directly behind the middle of the body. In *B. stylata*, a paired musculus longitudinalis dorsalis (musculus longitudinalis V) is also present (Fig. 1A, B) running between the head and the last foot pseudosegment, where it attaches to the musculus circumpedalis. As can be seen, the presence of this paired muscle has been demonstrated for different taxa in Ploima, Gnesiotrocha and Bdelloidea. Given its distribution, this dorsal longitudinal muscle pair also represents a ground pattern feature of Rotifera and apparently a plesiomorphic character in *B. stylata*. However, we are not convinced that the muscle pair is homologous with the dorsolateral muscles of *P. reinhardti* and *P. daphnicola* as assumed by Riemann et al. (2008) because (1) these muscles are orientated dorsolaterally and not dorsally in these species and (2) several longitudinal muscles are present in an even more dorsal position in *P. reinhardti*, *P. daphnicola* and several other rotifer species that we assume to be homologous with the muscoli longitudinales dorsales in *B. stylata*. We therefore suggest naming the dorsolateral muscles found in *P. reinhardti* and *P. daphnicola* muscoli longitudinales laterales superior (sg. musculus longitudinalis lateralis superior) to avoid confusion.

A second pair of dorsal longitudinal muscles centrally connecting the head and trunk have been identified in *E. senta* (musculus retractor centralis, see Remane 1929–1933); *S. baltica* (musculus retractor centralis, see

Peters 1931); *R. frontalis* (musculus retractor centralis, see Stoßberg 1932); *N. acuminata* (dorsal head retractor, see Sørensen et al. 2003); *P. reinhardti*, *P. fallaciosa* and *P. daphnicola* (dorsal head retractor see Sørensen 2005a); and *E. mucronatum* and *D. forcipatus* (musculus longitudinalis capitis, see Riemann et al. 2008). In *B. stylata*, a short paired musculus longitudinalis capitis (musculus longitudinalis IV) is present, running dorsally from the head the anterior part of the trunk as in *E. mucronatum* and *P. fallaciosa*. In *E. senta*, *R. frontalis* and *S. baltica*, the muscle pair extends from the head to the midbody region, whereas it terminates behind the head in *P. reinhardti* and *P. daphnicola*. Interpreting the data on this muscle pair in other rotifers is ambiguous. Despite the different lengths, we consider all these paired dorsolongitudinal muscles to be homologous, with it being reasonable to assume that they are present in the stem lineage of Ploima. A paired dorsolongitudinal muscle may have evolved in the stem lineage of Monogononta (Riemann et al. 2008), but, without more data, further phylogenetic reconstructions are vague. Following this assumption, the presence of this musculus longitudinalis capitis in *B. stylata* is a plesiomorphic character.

However, in none of the hitherto investigated Rotifera species have we found convincing equivalents for the musculus longitudinalis III and musculus longitudinalis VI present in *B. stylata*. It is likely that musculus longitudinalis III corresponds to the musculus retractor ventralis pedalis found in *Brachionus calyciflorus* (see Stoßberg 1932) and *Euchlanis pellucida* (see Stoßberg 1932), but, without more complete data, any further evaluations would be very speculative.

The circular muscles in rotifers, unlike their longitudinal counterparts, are highly variable in size, orientation and completeness, making homology determination a much more difficult task. *B. stylata* shares the presence of a musculus circumpedalis (m. circularis VIII) with several other ploimid rotifer species such as *B. eudactylota*, *D. forcipatus*, *B. quadridentatus* (see Kotikova et al. 2001) and *P. reinhardti*. This observation supports the hypothesis of the musculus circumpedalis being a ground pattern feature in Ploima. Further assumptions remain ambiguous without more data on species of Bdelloidea and Gnesiotrocha.

Compared with other ploimid rotifer species, *B. stylata* is characterized by the absence of a number of both longitudinal and circular muscles. For instance, the species lacks a dorsolateral muscle pair (we here suggest the term musculus longitudinalis lateralis superior) that is reported, for example, in *C. natans* and *L. tecusa* (musculus retractor lateralis superior, see Remane 1929–1933); *P. daphnicola* and *P. reinhardti* (dorsolateral trunk retractor, see Sørensen 2005a); *T. patina* (dorsolateral corona retractor, see Sørensen 2005b); *F. novaezealandiae* (dorsolateral retractor, see



Hochberg and Gurbuz 2007); and *D. forcipatus* (musculus longitudinalis IV, see Riemann et al. 2008). *B. stylata* also lacks a lateral muscle pair (we suggest the term musculus longitudinalis lateralis medius) that is documented in species like *C. natans* (musculus retractor lateralis medius, see Remane 1929–1933); *P. daphnicola* (lateral trunk retractor, see Sørensen 2005a); *E. mucronatum* (musculus longitudinalis III, see Riemann et al. 2008); and *B. eudactylota* (musculus longitudinalis II, see Riemann et al. 2009). Finally, *B. stylata* lacks a distinct pars coronalis. According to Riemann et al. (2008), the pars coronalis is associated with the anterior margin of the rotatory organ and follows the course of the buccal field. The coronal sphincter is usually a very broad muscle that directly underlies the integument and encloses the head during longitudinal contraction of the animal. Although we found two small muscle pairs in the anterior corona region of *B. stylata* (arrow heads Figs. 6B, 7A), neither shows accordance in position, length, direction or function with the pars coronalis or coronal sphincter. However, *B. stylata* is not able to contract its head completely, making the absence of a coronal sphincter plausible.

Following the assumption of Riemann et al. (2008) that the pars coronalis and the coronal sphincter evolved in the stem lineage of Ploima or even Monogononta and that the dorsolateral muscle pair is a ground pattern feature for Ploima or even Rotifera, it is more plausible at the moment to assume that these elements of the somatic muscle system were lost secondarily in *B. stylata* rather considering their absence to be a plesiomorphic character for the species. But testing this hypothesis adequately will require (1) further studies on more rotifer species as well as (2) a well-supported hypothesis for the phylogenetic position of *Bryceella* within Ploima. Indeed, both requirements are essentially to support or disprove this or any further phylogenetic evaluation of the muscular character traits of *B. stylata*.

Regarding Proalidae, information on the somatic musculature hitherto exists for three species of *Proales* only (see Sørensen 2005a). With the present study, data on the musculature within another genus of Proalidae becomes available. Future research should aim to obtain equivalent data for the two remaining genera, *Wulfertia* and *Proalinopsis*. Such data would be useful for reconstructing the ground pattern of the family and determining if there are genus-specific or even species-specific patterns. At present, it is simply not possible to use the known information of the somatic musculature in either a larger systematic or even a more functionally orientated context. To date, only Kotikova et al. (2001) and Sørensen (2005b) have made statements about the possibility of species-specific muscle patterns in *Asplanchnopus multiceps* and *T. patina*, respectively. The x-shaped musculus longitudinalis ventralis in *B. stylata*

might represent another possible instance of a species-specific character, given that, to our knowledge, this trait has not been reported for any other species.

## 4.2. Comparison with previous descriptions

*B. stylata* was described relatively early in the 19th century by Milne (1886). Since then SEM pictures of different views of the trophi have been provided in the comprehensive study on taxonomy, ecology and morphology of Proalidae by De Smet (1996). Otherwise, only marginal morphological records of the species exist. Correct information on the number of pseudosegments is lacking in the literature: De Smet (1996) stated a trunk without pseudosegments whereas Koste and Shiel (1990) stated an imprecise number of (2–3) foot pseudosegments. Both the presence and number of longitudinal ridges and folds of the first trunk pseudosegment, which are clearly visible only in SEM images, have not been described correctly to date. Only Koste and Shiel (1990) reported longitudinal sulci for *B. stylata*, but on the folds and ridges are indicated imprecisely on previous drawings. The presence and position of the lateral antennae have not been mentioned previously because they are only just recognizable by differential interference contrast light microscopy (but more precisely by SEM). Similarly, the epidermal shield-like projection covering the dorsal antennae in *B. stylata* (Fig. 4C) is only clearly visible on SEM images and, to our knowledge, has not yet been reported for any other rotifer species so far. Finally, the light-refracting bodies in the head of *B. stylata* are not associated with the base of the styli as stated by Milne (1886), but instead with the brain-complex as indicated by the TEM sections (Fig. 4C). Milne considered these structures to be eyes, but they almost certainly represent parts of a glandular system (possibly subcerebral glands). Such a glandular system has also not yet been reported for *Bryceella*, but light-refracting bodies in the head of some species of *Enicentrum* have been interpreted as structures of subcerebral glands by De Smet (1997).

The SEM images of the trophi of *B. stylata* presented by the landmark studies of De Smet (1996) and Sørensen (2002) are generally of good quality and show different views of the trophi and a more life-like orientation of the unci than is visible on our images. However, our SEM analysis revealed the presence of a previously unnoticed hypopharynx. This is possibly a result of the less aggressive SDS/DTT we used for trophi preparation, the sodium hypochlorite used by De Smet (1996) and Sørensen (2002) often being more aggressive on less cuticularized trophi structures. Both authors clearly show the presence of the accessory toothlet below the principal unci tooth that we could not present so clearly

due to the position of the trophi on the SEM stubs. Additionally, the studies of De Smet (1996) and Sørensen (2002) show the paired subuncus structure below the uncus of *B. stylata* in a more life-like orientation. Similar structures have been found in several other rotifer species with minor peculiarity such as *Brachionus plicatilis*, see Kleinow et al. (1990); *E. senta*, *Platyonus patulus*, *P. reinhardti* and *Brachionus bidentatus* (see Sørensen 2002); *Conochilus hippocrepis* (see Segers and Wallace 2001); *Pompholyx sulcata* (see De Smet 2005) and *Rhinoglena kutikova* (see De Smet and Gibson 2008). De Beauchamp (1909), Kleinow et al. (1990), De Smet (2005), De Smet and Gibson (2008) and other authors have used the term subuncus for the same structure, whereas Markevich and Kutikova (1989), De Smet (2001) and Sørensen (2002) refer to it as the “preuncus”. Concerning their wide distribution within Rotifera and the similarly in their location and shape, we consider the structures to be homologous with the structure found beneath the uncus in *B. stylata* and use the term subuncus. However, similar to the subuncus in *Brachionus amsterdamsis* (see Figs. 19 and 20 in De Smet 2001), the subuncus in *B. stylata* is very well developed, forming a large laminar structure with several teeth-like dentes protruding beneath the uncus. This development seems to be unique in rotiferan trophi morphology and we suggest the term “distal subuncus” for this characteristic subuncus to express its homology and diverseness to other subuncinal structures.

## Acknowledgements

We wish to thank the Evangelisches Studienwerk Villigst e.V. for financial support. We also gratefully acknowledge very helpful comments and criticism on the manuscript given by two anonymous reviewers. Comments on the manuscript by Olaf R.P. Bininda-Emonds and editorial remarks by Martin Vinther Sørensen are very much appreciated.

## References

- De Beauchamp, P.M., 1909. Recherches sur le rotifers: les formations tégumentaires et l'appareil digestif. Arch. Zool. Exp. Paris 10, 1–410.
- De Smet, W.H., 1996. Rotifera 4: The Proalidae (Monogononta). In: Dumont, H.J., Nogrady, T. (Eds.), Guides to the Identification of the Microinvertebrates of the Continental Waters of the World. SPB Academic Publishing BV., Amsterdam, pp. 1–102.
- De Smet, W.H., 1997. Rotifera 5: The Dicranophoridae. In: Dumont, H.J., Nogrady, T. (Eds.), Guides to the Identification of the Microinvertebrates of the Continental Waters of the World. SPB Academic Publishing BV., Amsterdam, pp. 1–325.
- De Smet, W.H., 1998. Preparation of rotifer trophi for light and scanning electron microscopy. Hydrobiologia 387–388, 117–121.
- De Smet, W.H., 2001. Some Rotifera from Ile Amsterdam (Terres Australes et Antarctiques Françaises), with description of *Brachionus amsterdamsis* sp. nov. (Monogononta: Brachionidae). Ann. Limnol. 37, 9–20.
- De Smet, W.H., 2005. Study of the trophi of *Testudinella* Bory de St. Vincent and *Pompholyx* Gosse (Rotifera: Testudinellidae) by scanning electron microscopy. Hydrobiologia 546, 203–211.
- De Smet, W.H., Gibson, A.E., 2008. *Rhinoglena kutikova* n. sp. (Rotifera: Monogononta: Epiphanidae) from the Bunger Hills, East Antarctica: a probable relict species that survived Quaternary glaciations on the continent. Polar Biol. 31, 595–603.
- Hlava, S., 1905. Beiträge zur Kenntnis der Rädertiere: Über die Anatomie von *Conochiloides natans*. Z. Wiss. Zool. 80, 282–326.
- Hochberg, R., Litvaitis, M.K., 2000. Functional morphology of the muscles in *Philodina* sp. (Rotifera: Bdelloidea). Hydrobiologia 432, 57–64.
- Hochberg, R., Gurbuz, O.A., 2007. Functional morphology of somatic muscles and anterolateral setae in *Filinia novaezealandiae* Shiel and Sanoamuang, 1993 (Rotifera). Zool. Anz. 246, 11–22.
- Kleinow, W., Klusemann, J., Wratil, H., 1990. A gentle method for the preparation of hard parts (trophi) of the mastax of rotifers and scanning electron microscopy of the trophi of *Brachionus plicatilis* (Rotifera). Zoomorphology 109, 329–336.
- Koste, W., Shiel, J., 1990. Rotifera from Australian inland waters. VI. Proalidae, Lindiidae (Rotifera: Monogononta). Trans. R. Soc. S. Aust. 114, 129–143.
- Kotikova, E.A., Raikova, O.J., Flyatchinskaya, L.P., Reuter, M., Gustafsson, M.K.S., 2001. Rotifer muscles as revealed by phalloidin-TRITC staining and confocal scanning laser microscopy. Acta Zool. 82, 1–9.
- Kotikova, E.A., Raikova, O.J., Flyatchinskaya, L.P., 2006. Study of architectonics of rotifer musculature by the method of fluorescence with use of confocal microscopy. J. Evol. Biochem. Phys. 42, 89–97.
- Markevich, G.I., Kutikova, L.A., 1989. Mastax morphology under SEM and its usefulness in reconstructing phylogeny and systematics. Hydrobiologia 186–187, 285–289.
- Martini, E., 1912. Studien über die Konstanz histologischer Elemente. III. *Hydatina senta*. Z. Wiss. Zool. 102, 425–645.
- Melone, G., 1998. The rotifer corona by SEM. Hydrobiologia 387–388, 131–134.
- Milne, W., 1886. On the defectiveness of the eye-spot as a means of generic distinction in the Philodinaea. Proc. Glasgow Phil. Soc. 17, 134–145.
- Peters, F., 1931. Untersuchungen über die Anatomie und Zellkonstanz von *Synchaeta* (*S. grimpei* REM., *S. baltica* EHRB., *S. tavina* Hood und *S. triophthalma* Laut.). Z. Wiss. Zool. 139, 1–119.
- Remane, A., 1929–1933. Rotatoria. In: Bronn's Klassen und Ordnungen des Tier-Reichs Bd. 4, Abt. II/1, pp. 1–577.
- Riemann, O., Martínez Arbizu, P., Kieneke, A., 2008. Organisation of body musculature in *Enicentrum mucronatum*

- Wulfert, 1936, *Dicranophorus forcipatus* (O.F. Müller, 1786) and in the ground pattern of Ploima (Rotifera: Monogononta). Zool. Anz. 247, 133–145.
- Riemann, O., Wilts, E.F., Ahlrichs, W.H., Kieneke, A., 2009. Body musculature of *Beauchampiella eudactylota* (Gosse, 1886) (Rotifera: Euchlanidae) with additional new data on the trophi an overall morphology. Acta Zool. 90, 265–274.
- Santo, N., Fontaneto, D., Fascio, U., Melone, G., Caprioli, M., 2005. External morphology and muscle arrangement of *Brachionus ureolaris*, *Floscularia ringens*, *Hexarthra mira* and *Notommata glyphura* (Rotifera, Monogononta). Hydrobiologia 546, 223–229.
- Segers, H.H., Wallace, R.L., 2001. Phylogeny and classification of the Conochilidae (Rotifera, Monogononta, Flosculariacea). Zool. Scr. 30, 37–48.
- Sørensen, M.V., 2002. On the evolution and morphology of the rotiferan trophi, with a cladistic analysis of Rotifera. J. Zool. Syst. Evol. Res. 40, 129–154.
- Sørensen, M.V., Funch, P., Hooge, M., Tyler, S., 2003. Musculature of *Notholca acuminata* (Rotifera: Ploima: Brachionidae) revealed by confocal scanning laser microscopy. Invertebr. Biol. 122, 223–230.
- Sørensen, M.V., 2005a. Musculature in three species of *Proales* (Monogononta, Rotifera) stained with phalloidin-labelled fluorescent dye. Zoomorphology 124, 47–55.
- Sørensen, M.V., 2005b. The musculature of *Testudinella patina* (Rotifera: Flosculariacea), revealed with CLSM. Hydrobiologia 546, 231–238.
- Stoßberg, K., 1932. Zur Morphologie der Rädertiergattung *Euchlanis*, *Brachionus* und *Rhinoglena*. Z. Wiss. Zool. 142, 313–424.
- Wilts, E.F., Bininda-Emonds, O.R.P., Ahlrichs, W.H., 2009. Comparison of the predatory rotifers *Pleurotrocha petromyzon* (Ehrenberg, 1830) and *Pleurotrocha sigmoidea* Skorikov, 1896 (Rotifera: Monogononta: Notommatidae) based on light and electron microscopic observations. Zootaxa 2130, 1–20.